Turk J Chem
30 (2006) , 691 – 701.

A New Method for the Preparation of Pyridazine Systems: Experimental Data and Semiempirical PM3 Calculations

Dilek ÜNAL[1]*, Emin SARIPINAR[2], Yunus AKÇAMUR[3]
[1] *Erciyes University, Department of Chemistry, 38039, Kayseri-TURKEY*
e-mail: dilekunal@erciyes.edu.tr
[2] *Erciyes University, Department of Chemistry, 38039, Kayseri-TURKEY*
[3] *Erciyes University, Yozgat Faculty of Arts & Sciences, Department of Chemistry, 66200, Yozgat-TURKEY*

Received 21.06.2004

The reactions of 4-benzoyl-5-phenyl-2,3-furandione (**1a**) and 4-(4-methoxybenzoyl)-5-(4-methoxyphenyl)-2,3-furandione (**1b**) with acyl hydrazines (**2**) (namely hydrazides) are reported. From these reactions, novel pyridazinone systems (**3a-g**) are obtained as well as the cyclization product of **3g** at high temperature (**4**). The electronic properties and conformational parameters for these molecules, such as bond lengths, bond angles, torsion angles and atom charges, are calculated with a semiempirical PM3 method. In order to determine the mechanism of the reaction between the model furandion (**R1**) and formic hydrazide (**R2**), the electronic properties, conformational parameters and imaginary frequencies of the reactants, transition states and intermediates are calculated at the same level of theory as well.

Key Words: Hydrazide, furandione, pyridazine, semiempirical, PM3.

Introduction

Pyridazine systems have received considerable attention in recent decades due to their biological activities as antiplatelet agents[1], inhibitors of glycogen synthase kinase[2], antimicrobial agents[3] etc., and these pharmacological activities have inspired chemists to synthesize substituted pyridazine systems in order to explore the usefulness of this heterocyclic template. As a result, several attempts have been made to synthesize and characterize compounds containing pyridazine functionality. Furandiones of type **1** have been successfully used in the synthesis of heterocyclic systems by the reactions of various nucleophiles[4−17] for a long time. Our approach to pyridazine systems was achieved by the reaction of the title compounds 4-benzoyl-5-phenyl-2,3-furandione (**1a**) and 4-(4-methoxybenzoyl)-5-(4-methoxyphenyl)-2,3-furandione (**1b**) with various acyl hydrazines (or hydrazides namely). In this paper, the synthesis and characterization of the pyridazine-3-one derivatives **3a-g** are presented (Scheme 1). This study also includes a cyclization reaction of a pyridazine derivative, **3g**, to a pyridazino triazine system **4** (Scheme 4).

*Corresponding author

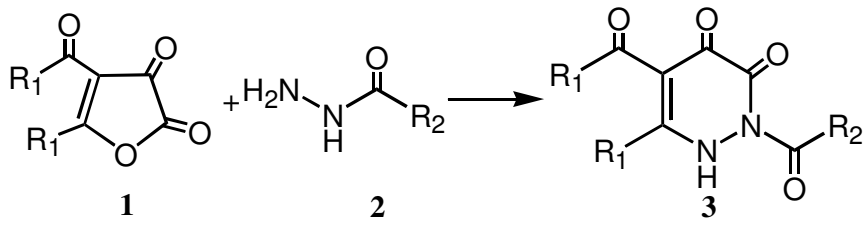

1 **2** **3**

1	$\mathbf{R_1}$
a	-Ph
b	-Ar

2	$\mathbf{R_2}$
a	$-CH_3$
b	-Ph
c	-H
d	$-CO-NH-NH_2$

3	$\mathbf{R_1}$	$\mathbf{R_2}$
a	-Ph	$-CH_3$
b	-Ph	-Ph
c	-Ar	$-CH_3$
d	-Ar	-H
e	-Ar	-Ph
f	-Ph	$-CO-NH-NH_2$
g	-Ar	$-CO-NH-NH_2$

Ar: *p*-CH_3-O-C_6H_4-

Scheme 1. The general scheme for the reaction of furan-2,3-diones (**1a,b**) with acyl hydrazides (**2a-d**).

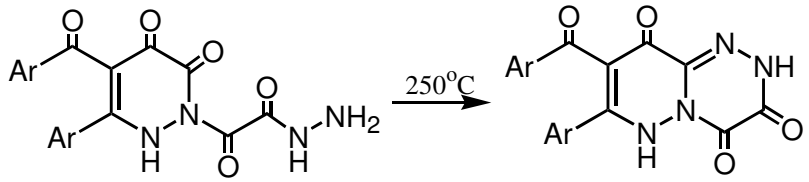

3g **4**

Scheme 2. Scheme for the hydrolysis reaction of **3g**.

To study the mechanism of the reaction of the model compounds, 4-formyl-2,3-furandione **R1** and formic hydrazide **R2**, all calculations were carried out by means of a semiempirical PM3 method with full geometry optimization for reactants, products and intermediates[18]. The PM3 calculations were carried out using the SPARTAN software package[19]. Transition structures were located using a linear synchronous transition method within SPARTAN, and confirmed by vibrational analysis (computation of force constants analytically), and characterized by the corresponding imaginary vibration modes and frequencies. Vibrational mode analysis was systematically carried out to confirm that on a potential energy surface all optimized geometries correspond to a local minimum that has no imaginary frequency mode. Model compounds with aryl and phenyl groups substituted by hydrogen atoms were used in the theoretical calculations in order to make the calculations easier. The results of the calculations (the formation enthalpies, ΔH_f in kcal.mol^{-1}, dipole moments, μ, in debyes, the highest and lowest molecular orbital energies, E_{HOMO} and E_{LUMO}, in eV, and lowest or imaginary frequencies, in cm^{-1}) are given in Table 1.

Experimental

Solvents were dried by refluxing with the appropriate drying agents and distilled before use. Melting points were determined on a Buchi 510 and were uncorrected. Elemental analyses were performed on an EA-

1100 Elemental Analyzer. The IR spectra were recorded on a Shimadzu Model 435 V-04 spectrometer, using potassium bromide disks. The ^{1}H NMR spectra were recorded on a Gemini-Varian 200 MHz ^{1}H NMR Spectrophotometer and ^{13}C NMR spectra were recorded on Gemini Varian 50 MHz ^{13}C NMR Spectrophotometer using DMSO as an internal standard. The chemical shifts are reported in ppm from tetramethylsilane and given in δ units. All experiments were followed using DC Alufolien Kieselgel 60 F 254 Me4rc and Camag TLC lamp (254/366 nm).

2-Acetyl-5-benzoyl-6-phenyl-1,2-dihydro-pyridazine-3,4-dione (3a)

An equimolar mixture of 4-benzoyl-5-phenylfuran-2,3-dione (**1a**) (0.56 g, 0.02 mol) and acetic hydrazide (**2a**) (0.15 g, 0.02 mol) was refluxed in toluene (30 mL) for 4 h. After the solvent was removed by evaporation, the oily residue was treated with diethyl ether overnight. The crude product formed was crystallized from acetic acid to give 60% yield of **3a**; mp: 349.5 °C; IR: 3400 (-N-H); 1715, 1640, (-C=O), 1440 (-C=N); 1380 (C=C), ^{1}H NMR (200 MHz, DMSO): δ 2.40 (s, CH3, 6H); 7.758-7.232 (m., Ar-H, 10H); 9.82 (s, enol form, -OH, 1H); 11.032 (s, keto form, -NH, 1H); ^{13}C NMR (DMSO): δ 180.30 (t, ArCO); 178.93 (s, C3); 170.53 (s, C14); 160.84 (s,C5); 158.02 (s, C2); 138.70-127.74 (m, Ar. C); 114.33 (s, C4); 21.41 (s, CH_3). Anal. Calcd. for $C_{19}H_{14}N_2O_4$ (334.33 g/mol): C, 68.26; H, 4.22; N, 8.38. Found: C, 68.19; H, 4.19; N, 8.03.

3,5-Dibenzoyl-6-phenyl-1,2-dihydro-pyridazine-3,4-dione (3b)

Compound **3b** was prepared according to the general procedure above by the reaction of **1a** and benzoic hydrazide (**2b**) with a reflux time of 2 h, resulting in 40% yield; mp: 400 °C; IR: 3450 (-N-H); 2400 (C-H, arom.); 1730, 1690, 1675, 1580 (-C=O); 1430 (C=N); 1380 (-C=C-, arom.), ^{1}H NMR (200 MHz, DMSO): δ 7.84-7.25 (m, Ar-H, 15H); 11.258 (s, keto form, -NH, 1H); ^{13}C NMR (DMSO): δ 189.16 (t, ArCO): 168.44 (s, C3); 163.82 (s, C14); 156.82 (s, C5); 150.62 (s, C2); 136.44-124.02 (m, Ar.C); 118.22 (s, C4). Anal. Calcd. for $C_{24}H_{16}N_2O_4$ (396.36 g/mol): C, 72.73; H, 4.04; N, 7.07. Found: C, 73.05; H, 3.76; N, 7.18

2-Acetyl-5-(4-methoxy-benzoyl)-6-(4-methoxy-phenyl)-1,2-dihydro-pyridazine-3,4-dione (3c)

Compound **3c** was prepared according to the general procedure above by the reaction of **1b** and acetic hydrazide (**2c**) with a reflux time of 2 h, resulting in 60% yield; mp: 387 °C; IR: 3400 (-N-H); 2400 (C-H, arom.); 1720, 1650 (-C=O); 1440 (C=N); 1380 (-C=C-, arom.), ^{1}H NMR (200 MHz, DMSO): δ 2.31 (s, 3H); 3.50 (s, 6H); 6.99-8.04 (m, Ar-H, 8H); 11.258; ^{13}C NMR (DMSO): δ 189.64 (t, ArCO): 185.54 (s, C3); 166.43 (s, C14); 162.80 (s, C5); 155.16 (s, C2); 164.14-118.52 (m, Ar.C); 116.38 (s, C4); 20.18 (s, CH_3). Anal. Calcd. for $C_{21}H_{18}N_2O_6$ (396.36 g/mol): C, 63.69; H, 4.57; N, 7.11. Found: C, 64.80; H, 4.29; N, 7.39

4-(4-Methoxy-benzoyl)-3-(4-methoxy-phenyl)-5,6-dioxo-5,6-dihydro-2H-pyridazine-1- carbaldehyde (3d)

Compound **3d** was prepared according to the general procedure above by the reaction of **1b** and acetic hydrazide (**2a**) with a reflux time of 4 h, resulting in 65% yield; mp: 333 °C; IR: 3400 (-N-H); 2400 (C-H, arom.); 1715, 1650, 1590 (-C=O); 1435 (C=N); 1380 (-C=C-, arom.), 1240 (-C-H); ^{1}H NMR (200 MHz, DMSO): δ 3.51 (s, 6H); 6.98-7.92 (m, Ar-H, 8H); 10.84 (s, 1H); ^{13}C NMR (DMSO): δ 188.29 (t, ArCO):

178.91 (s, C3); 160.80 (s, C14); 153.56 (s, C5); 151.56 (s, C2); 164.48-112.09 (m, Ar.C); 108.21 (s, C4). Anal. Calcd. for $C_{20}H_{16}N_2O_6$ (380.35 g/mol): C, 63.16; H, 4.21; N, 7.37. Found: C, 63.45; H, 4.09; N, 7.15.

2-Benzoyl-5-(4-methoxy-benzoyl)-6-(4-methoxy-phenyl)-1,2-dihydro-pyridazine-3,4-dione (3e)

Compound **3e** was prepared according to the general procedure above by the reaction of **1b** and acetic hydrazide (**2b**) with a reflux time of 4 h, resulting in 65% yield; mp: 343.8 °C; IR: 3400 (-N-H); 2000 (C-H, arom.); 1660, 1630, 1590 (-C=O); 1440 (C=N); 1380 (-C=C-, arom.); ^{1}H NMR (200 MHz, DMSO): δ 3.48-3.52 (d, 6H); 5.18 (s, NH); 6.89-7.97 (m, Ar-H, 13H); ^{13}C NMR (DMSO): δ 188.68 (t, ArCO): 181.19 (s, C3); 165.18-111.48 (m, Ar.C); 156.27 (s, C5); 157.09 (s, C14); 151.24 (s, C2); 102.99 (s, C4); 56.18 (s, -OCH_3). Anal. Calcd. for $C_{26}H_{20}N_2O_6$ (456.45 g/mol): C, 68.40; H, 4.37; N, 6.14. Found: C, 68.47; H, 4.32; N, 6.42.

(4-Benzoyl-5,6-dioxo-3-phenyl-5,6-dihydro-2H-pyridazine-1yl)-oxo-acetic acid hydrazide (3f)

Compound **3f** was prepared according to the general procedure above by the reaction of **1a** and acetic hydrazide (**2d**) with a reflux time of 4 h, resulting in 45% yield; mp: 390 °C; IR: 3450 (-N-H); 2000 (C-H, arom.); 1660, 1630, 1615, 1590, (-C=O); 1440 (C=N); 1375 (-C=C-, arom.); ^{1}H NMR (200 MHz, DMSO): δ 5.37 (s, NH2); 6.65 (-OH, enol form); 7.53-7.99 (m, Ar-H, 15H); ^{13}C NMR (DMSO): δ 193.52 (t, ArCO): 176.18 (s, C3); 164.48 (s, C14); 159.72 (s, C5); 151.62 (s, C2); 137.18-130.19 (m, Ar.C); 109.21 (s, C4). Anal. Calcd. for $C_{19}H_{14}N_4O_5$ (378.34 g/mol): C, 60.32; H, 3.71; N, 14.82. Found: C, 60.48; H, 3.87; N, 15.11.

[4-(4-Methoxy-benzoyl)-3-(4-methoxyphenyl)-5,6-dioxo-5,6-dihydro-2H-pyridazine-1-yl]-oxo-acetic acid hydrazide (3g)

Compound **1b** (0.66 g) and oxalyl dihydrazide (**2d**) (0.12 g) were mixed until a homogeneous mixture was obtained and the mixture was put in an 850 W microwave oven at 50 °C until the color ceased to change. The reaction ended after no more gas was present. The oily product was treated with dry ethyl ether to give an orange colored crude product, which was recrystallized from acetic acid and allowed to dry on P_2O_5, resulting in 35% yield; mp: 236 °C; IR: 3450 (-N-H); 2000 (C-H, arom.); 1660, 1640, 1590, (-C=O); 1460 (C=N); ^{1}H NMR (200 MHz, DMSO): δ 3.85 (s, 6H); 4.03 (s, NH_2); 6.73-7.78 (m, Ar-H, 8H); ^{13}C NMR (DMSO): δ 192.24 (t, ArCO); 188.62 (s, C15); 185.98 (s, C3); 165.04 (s, C5); 161.79 (s, C14); 159.52 (s, C2); 128.24-133.16 (m, Ar.C); 115.67 (s, C4). Anal. Calcd. for $C_{21}H_{18}N_4O_7$ (438.39 g/mol): C, 57.53; H, 4.14; N, 12.78. Found: C, 57.48; H, 4.11; N, 12.32.

8-(4-Methoxy-benzoyl)-7-(4-methoxy-phenyl)-2H, 6H-pyridazino-[6,1-c] [1,2,4]-triazine-3,4,9-trion (4)

Compound **3g** (0.2 g) was put in the 850 W microwave oven at 250 °C for 30 min and the reaction ended after no more color change and gas were observed. The obtained oily product was treated with dry ethyl ether to give an orange colored crude product, which was purified by washing with benzene and diethyl ether and allowed to dry on P_2O_5, resulting in 60% yield; mp: 255 °C; IR: 3450 (-N-H); 2000 (C-H, arom.); 1660, 1640, 1600 (-C=O); 1460 (C=N); 1380 (-C=C-, arom.); ^{1}H NMR (200 MHz, DMSO): δ 3.79 (s, 6H);

6.77-7.96 (m, Ar-H, 8H); ^{13}C NMR (DMSO): δ 188.47 (t, ArCO): 182.26 (s, C3); 172.63 (s, C15); 165.16 (s, C5); 164.82-115.12 (m, Ar.C); 151.19 (s, C2); 150.88 (s, C14). Anal. Calcd. for $C_{21}H_{16}N_4O_6$ (420.37 g/mol): C, 60.00; H, 3.801; N, 13.33. Found: C, 59.48; H, 4.11; N, 13.32.

Results and Discussion

The α,β-unsaturated carbonyl compounds **1a** and **1b** include a C=C bond, which is conjugated to the carbonyl functionalities. In alkenes C=C bonds are not polar, but when there is an electron attractive group aligned, the bond becomes polar. In compounds **1a** and **1b**, the polar carbonyl groups C8-O10 and C3-O7 shift the double bond electrons of the C4=C5 to the O7 and O10, resulting in a charge decrease in the C5 atoms, which makes C5 open to the attack of nucleophiles. As a result, a simple procedure for the generation of pyridazine dione systems is the Michael type of addition of the highest electron density N1 atom of the hydrazide to the C5 atom of the furandione system, leading to the information of a zwitterion, which has higher energy and corresponds to an intermediate on the potential energy surface.

Treatment of the yellow 4-benzoyl-5-phenylfuran-2,3-dione **1a** and 4-(4-methoxybenzoyl)-5-(4-methoxyphenyl)-2,3-dihydro-2,3-dione **1b** with hydrazides **2a-d** at 60-120 °C furnishes the corresponding orange colored pyridazine-3,4-diones **3a-g**. The reaction equations are shown in Scheme 1. The further cyclization of **3g** gives the orange colored pyridazino triazine system **4** (see Scheme 2). The structures of **3a-g** and **4** were confirmed by elemental analysis, and IR, ^{1}H NMR and ^{13}C NMR data.

The reaction mechanisms for selected model structures were determined using PM3 calculations. The study includes a conformational analysis of the reactants, transition structures and products. The main stages of the reaction mechanism are shown in Scheme 3, and the spatial dispositions of the atoms for the reactants **R**, intermediates **IN**, transition states **TS** and products **P** are shown in Figure 1.

Calculations to elucidate the reaction mechanisms of the furan-2,3-dione systems with hydrazides show that the reaction mechanism involves several steps. The reaction starts with the interaction of the atoms N12 and C5. Until the distance of the C5 and N12 becomes 2.122 Å, the 2 atoms show no interaction. In this case, the formation enthalpies of the 2 reactants are the sum of the individuals. As the distance between the mentioned atoms decreases, the positive charge of the C5 atom of the **R1** originates the attraction of the negative charge of the N12 atom of **R2** itself. It may be suggested that it is precisely the HOMO-LUMO and the interaction of their constituent C5 and N12 that is the first stage of the reaction. The frontier orbitals' localization at the reaction center forces the orbitals' energy levels to approach each other. The LUMO of **R1** and the HOMO of **R2** attract each other, and as a result of this attraction the system passes into the transition structure, **TS1**. The LUMO of **R1** and the HOMO of **R2** have the smallest energy difference and polarized orbitals (**R1** HOMO: -10.967 eV, LUMO: -1.682 eV; **R2** HOMO: -9.913 eV, LUMO: 0.700 eV). As the orbital coefficients of the 2 molecular orbitals are close to each other, the attraction will be easier. The LUMO of furan π^*, which is a π antibonding orbital, is strongly polarized to C5 and is relatively low in energy, at least compared with π^* orbital of the hydrazide, **R2**. Thus the larger the coefficients of the C5-Px orbital means that the carbonyl π^* orbital of **R1** will interact strongly with the HOMO of hydrazide (-9.91 eV, see Table 1).

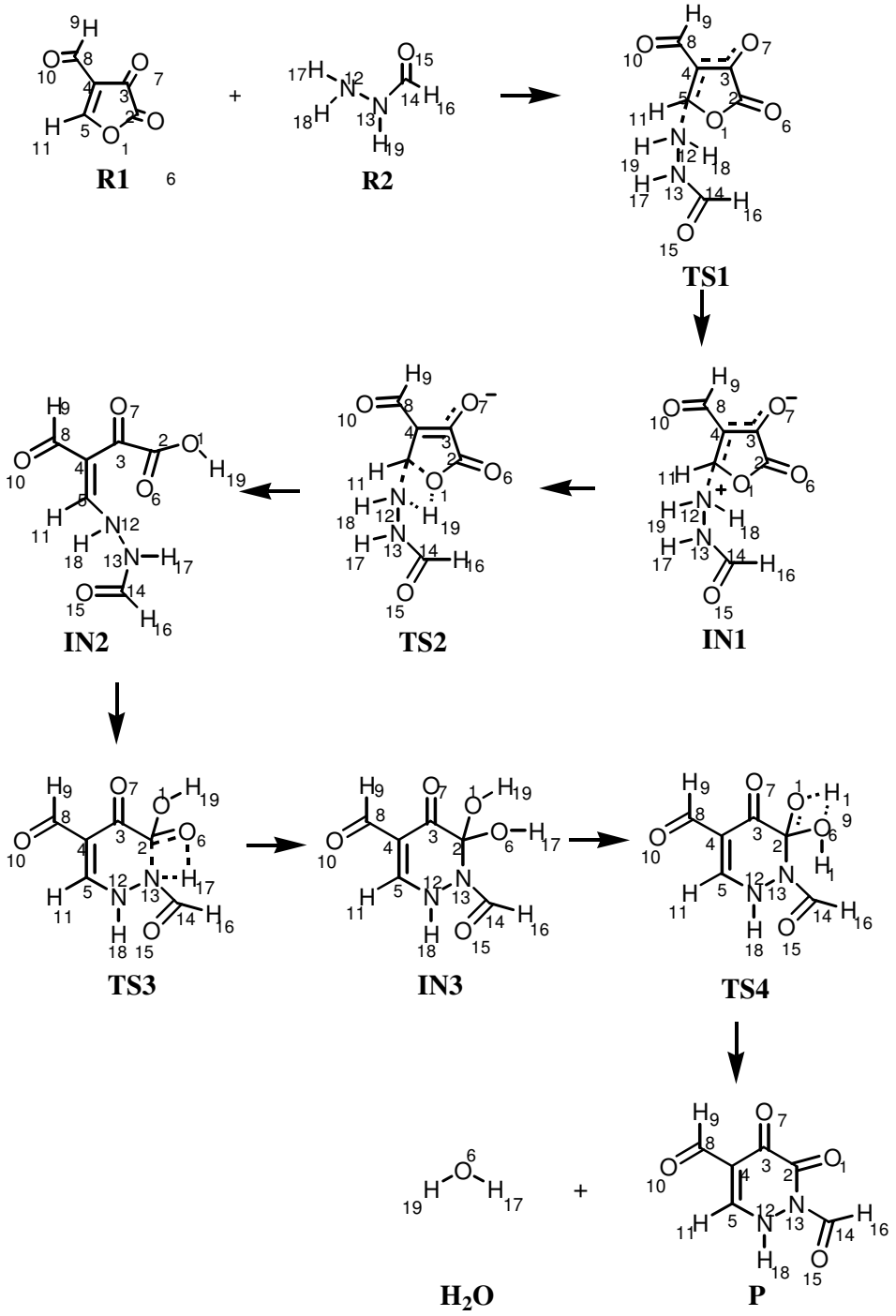

Scheme 3. Scheme for the reaction mechanism of **R1** and **R2**.

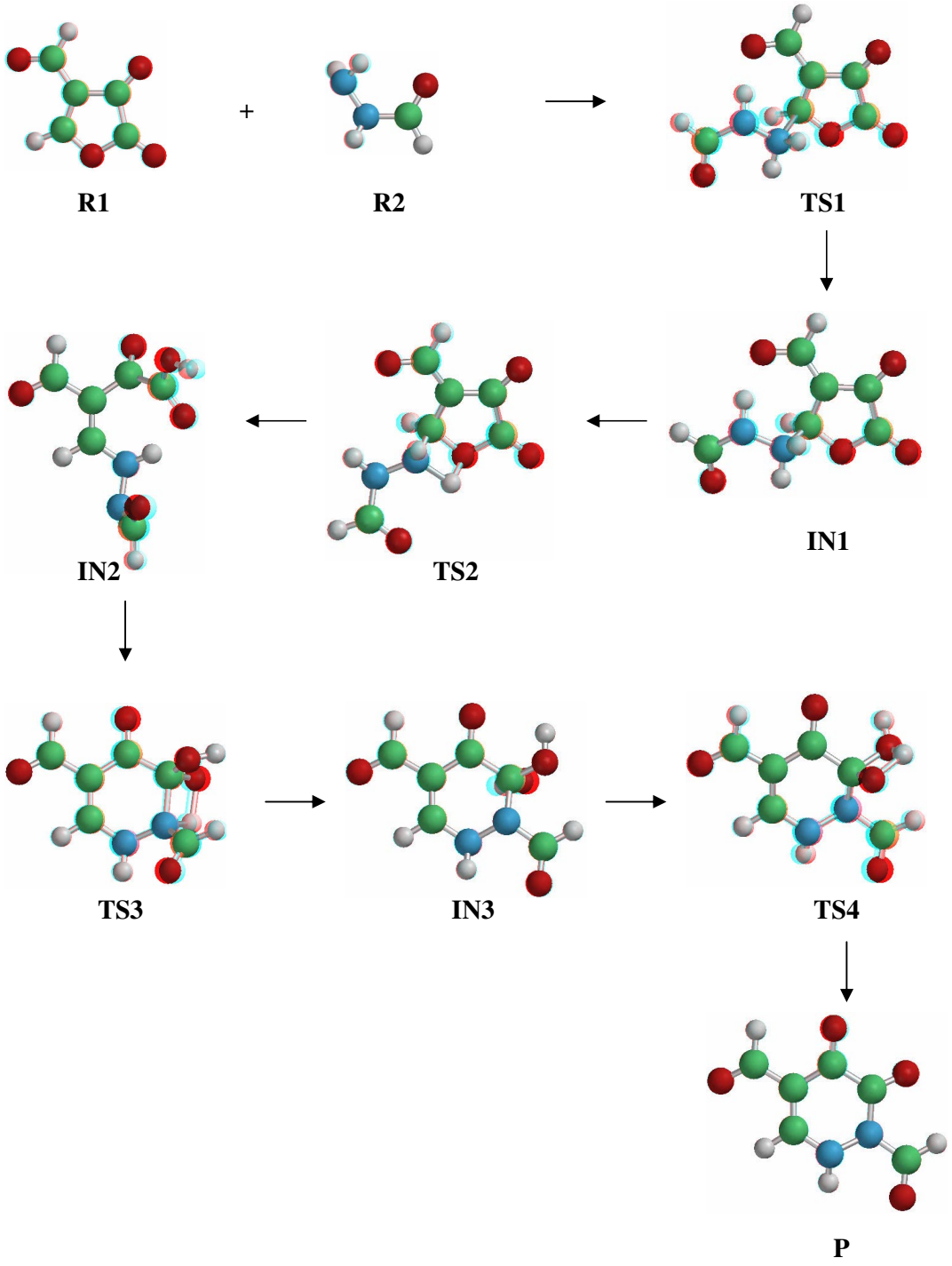

Figure 1. The spatial arrangements of the atoms for the reactants, transition states, intermediates and product.

Table 1. Calculated (PM3) relative energies, dipole, HOMO and LUMO orbital energies and imaginary frequencies for the reactants, transition states, intermediates and product.

Compound	ΔE **(kcal/mol)**	μ (debye)	E_{HOMO}	E_{LUMO}	υ (cm^{-1})
R1	-117.453	1.980	-10.967	-1.682	-
R2	-16.423	1.823	-9.913	0.700	-
(R1+R2)$_{rel}$	0.000	-	-	-	-
TS1	7.086	2.052	-9.814	-1.317	-285.42
IN1	-0.575	6.487	-9.214	-1.000	-
TS2	46.317	7.152	-8.748	-0.900	-2014.35
IN2	-17.512	3.711	-9.689	-0.725	-
TS3	34.877	4.426	-10.093	-1.177	-1925.56
IN3	-22.795	0.895	-9.703	-1.222	-
TS4	27.162	3.658	-9.528	-1.026	-106.40
P	38.765	2.176	-9.553	-1.383	-
P+H_2O	-14.662	-	-	-	-

The molecular planes of the reactants approach at an angle of 65.31° (see Table 2). The positive charge on the atom C5 increases from 0.219 ē to 0.316 ē in **R2** and **TS1** respectively, because of the C4-C5 double bond opening. The bond length of C4-C5 is 1.364 Å in **R1** and 1.390 Å in **TS1**, respectively, showing the transformation of this bond from a double bond to a single bond. The significant charge increase on O7 in **TS1** is due to the resonance structure of the **TS1** molecule in which the C3-C4 bond electrons are transferred directly to O7. The C5 and N12 atoms further approach until this distance 1.590 Å transfers the system into a zwitterion structure. The agreement in energy levels between **IN1** (ΔE_{rel} = -0.868 kcal.mol^{-1}) and **TS1** (ΔE_{rel} = 6.793 kcal.mol^{-1}) leads to the assumption that these molecule structures are similar. **IN1** exists as an unstable reaction intermediate, i.e. a local minimum on the potential energy surface. The value of valence angle of O1-C5-C4 at **IN1** is close to that in sp^3 hybridized carbon (108.67°) and the C4-C5 bond length increases to 1.469 Å. The positive charge on the C5 atom decreases because of the N12 atom's giving its lone pair of electrons completely to C5. The charge on the N12 atom at **IN1** is calculated as 0.561 ē, which proves that the structure is a high-energy zwitterion (see Table 3).

Table 2. Optimized geometrical parameters of reactants, transition states, intermediates and product.

Bond Lengths (Å)	**R1+R2**	**TS1**	**IN1**	**TS2**	**IN2**	**TS3**	**IN3**	**TS4**	**P**
C4-C5	1.364	1.390	1.469	1.470	1.360	1.351	1.360	1.361	1.357
O1-C5	1.372	1.377	1.419	1.462	-	-	-	-	-
C5-N12	-	2.122	1.590	1.514	1.407	1.412	1.397	1.401	1.401
O1-H19	-	-	-	1.326	0.953	0.953	0.948	-	-
C3-O7	1.202	1.205	1.211	1.213	1.211	1.212	1.215	1.212	1.212
N12-N13	1.439	1.456	1.479	1.457	1.447	1.471	1.470	1.467	1.467
C2-N13	-	-	-	-	-	1.666	1.508	1.449	1.449
O6-H17	-	-	-	-	-	1.477	0.950	0.951	0.951
13-H17	0.998	1.020	1.041	1.000	0.997	1.342	-	-	-
C2-O6	1.195	1.195	1.197	1.188	1.222	1.321	1.388	1.494	1.212
Bond Angles (°)									
C4-C5-O1	113.84	112.52	108.67	107.46	123.53	123.64	-	123.79	122.90
C5-N12-H19	-	110.12	109.74	81.29	-	-	-	-	-
O1-C2-O6	114.55	107.98	109.29	108.09	110.66	109.69	90.18	89.51	-
O1-C2-N13	-	-	-	-	-	109.03	112.10	115.64	11.87

Table 3. Mulliken charges of the selected atoms for the reactants, transition states, intermediates and product.

Atoms	**R1+R2**	**TS1**	**IN1**	**TS2**	**IN2**	**TS3**	**IN3**	**TS4**	**P**
O1	-0.206	-0.270	-0.290	-0.267	-0.267	-0.349	-0.320	-0.499	-0.292
C2	0.284	0.286	0.299	0.289	0.345	0.350	0.239	0.282	0.233
C3	0.336	0.359	0.388	0.414	0.374	0.338	0.309	0.345	0.336
C4	-0.453	-0.580	-0.745	-0.738	-0.433	-0.360	-0.418	-0.414	-0.399
C5	0.219	0.316	0.147	0.210	0.062	-0.002	0.031	0.032	0.014
O6	-0.221	-0.231	-0.262	-0.229	-0.400	-0.550	-0.304	-0.307	-0.359
O7	-0.226	-0.256	-0.312	-0.332	-0.265	-0.264	-0.297	-0.322	-0.257
C8	0.369	0.410	0.422	0.408	0.354	0.344	0.351	0.356	0.351
O9	-0.322	-0.388	-0.486	-0.454	-0.333	-0.329	-0.355	-0.340	-0.330
H10	0.069	0.070	0.071	0.057	0.061	0.078	0.073	0.070	0.075
H11	0.151	0.128	0.103	0.121	0.140	0.139	0.140	0.139	0.142
N12	-0.026	0.025	0.561	0.092	0.000	0.059	0.091	0.117	0.104
N13	-0.107	-0.191	-0.317	-0.136	-0.098	-0.185	-0.182	-0.192	-0.175
C14	0.231	0.261	0.299	0.268	0.240	0.273	0.308	0.304	0.300
O15	-0.365	-0.363	-0.340	-0.336	-0.336	-0.279	-0.348	-0.336	-0.327
H16	0.084	0.096	0.121	0.108	0.091	0.120	0.122	0.101	0.126
H17	0.092	0.161	0.226	0.119	0.097	0.306	0.232	0.233	0.179
H18	0.048	0.056	0.060	0.090	0.135	0.092	0.105	0.100	0.100
H19	0.043	0.067	0.056	0.316	0.233	0.237	0.204	0.329	0.179

The transition from **IN1** to **IN2** occurs via the 4-membered cyclic transition state **TS2**, which is characterized by the imaginary frequency of value 285.42 cm^{-1}, produced by the approach of O1 to H19, resulting in simultaneous bond breakage. The torsion angle O1-C5-N12-H19 is calculated as -0.160° and the system is ready to pass to the next stage of the reaction at which H19 passes from N12 to O1. The tension of the 4-centered ring causes the transfer of the system to the intermediate to be achieved more easily.

The transition from **IN1** to **IN2** occurs via the **TS2** structure, which is characterized by the presence of a 4-membered cycle including O1-C5-N12-H19 atoms, produced by the approach of O1 to H19 until the distance 1.326 Å leading to the lone pair interaction of the O1 to H19, resulting in the bond cleavage of C5-O1. As the O1 interacts with H19, leading to a new bond formation, the O1-C5 bond length increases to 2.213 Å and weakens as a N12-H19 bond (1.492 Å). The imaginary frequency for **TS2** is 285.42 cm^{-1} and ΔE_{rel} for this structure is calculated as 46.024 $kcal.mol^{-1}$. Because of the tension of the 4-centered ring in the transition structure, the activation energy of the system from **IN1** to **IN2** is high, and the system readily transfers from the **TS2** structure to the intermediate. In the **TS2** structure, a high negative charge is concentrated on the O1 atom (-0.276 ē) and C4 (-0.738 ē) because of the resonance structures. The torsion angle of O1-C5-N12-H19 is calculated as -0.160° and so the system is ready to pass to the next stage of the reaction, that is, H19 passes from N12 to O1. The bond cleavage of O1-C5 results in an open-chain intermediate **IN2** (ΔE_{rel}= -17.805 $kcal.mol^{-1}$). In this structure C4-C5 and O7-C5 bonds are rearranged to double bonds; thus the value of the bond length decreases after the formation of a new bond O1-H19 (0.953 Å). The C4-C5-N12 bond angle shows that C5 has a sp^2 character in this structure (123.53 Å).

When the distance between O6 and H17 becomes 1.477 Å there will be a simultaneous interaction between these atoms and between C2 and N13 (1.666 Å), resulting in the 6-membered pyridazine ring (υ = 2014.35 cm^{-1}) **TS3** (ΔE_{rel} = 34.583 $kcal.mol^{-1}$). The charge on O6 is calculated as -0.400 ē and -0.550 ē in **IN2** and **TS3**, respectively. This increase is due to the conversion of the C2=O6 double bond to a

single bond, and so the double bond electrons are directed towards O6. C2 is characterized as sp^2 in **IN2** and the value of the valence angle of O1-C2-O6 is 117.24° in **IN2**. This value is 109.69° in **TS3** and C2 is characterized as sp^3 in this structure. The torsion angle of C2-O6-H17-N13 shows that the bonding atoms of the 4-membered cyclic structure are situated in parallel, and thus in the same plane (-4.25°).

The system conversion from **TS3** to the intermediate **IN3** (ΔE_{rel} = -23.088 kcal.mol^{-1}) occurs by the bond cleavage of N13-H17 and the formation of 2 new bonds C2-N13 (1.508 Å) and O6-H17 (0.950 Å). Concurrent with the sp^3 hybridization of C2, the O1-C2-N13 bond angle is calculated as 112.10° and as a result of the single bond arrangement of the C2-O6 bond the bond length is calculated as 1.388 Å. The torsion angle of C3-C4-C5-N12 shows the system's planarity (-6.75°).

In the following step, negatively charged O6 (-0.304 ē) attacks the O1 bonded H19 (0.204 ē) in order to actualize the H_2O separation, leading to a 4-membered transition state, **TS4** of imaginary frequency υ = 106.40 cm^{-1} (ΔE_{rel} = 28.869 kcal.mol^{-1}). The value of the bond angle O1-C2-O6 (89.51°) shows that the transition system is highly strained. The attachment of O6 to H19 causes a change in the C3-C2-O6-H17 torsion angle in the system (-41.98° at **IN3** and 13.27° at **TS4**) leading to transfer to the last product of the mechanism by the separation of the H_2O molecule.

Further separation of the H_2O molecule returns C2 to the state of sp^2 hybridization. The double bond reorganization and proton disconnection from C2 occurs by this in the system. At this final stage of the reaction mechanism, the pyridazine skeleton takes a planar configuration due to the π-conjunction in the system (C3-C4-C5-N12: 3.50°) and product **P** is obtained (ΔE_{rel} = 38.472 kcal.mol^{-1}). The bond lengths C2-N12 and C2-O1 are calculated as 1.401 Å and 1.212 Å, showing that the C2-N13 bond gains a completely single bond character, whereas the C2-O1 bond rearranges to a double bond. In the reaction product **P** a decrease in the charges is observed caused by the growth of π-conjunction in the heterocycle.

In Figure 2 the energy profile of the reaction of furandion with the hydrazide molecule by means of the interaction of C5 and N12 is shown. The transition state **TS3** possesses the greatest formation energy for the construction of **IN3** and thus is the rate determining step of this reaction mechanism.

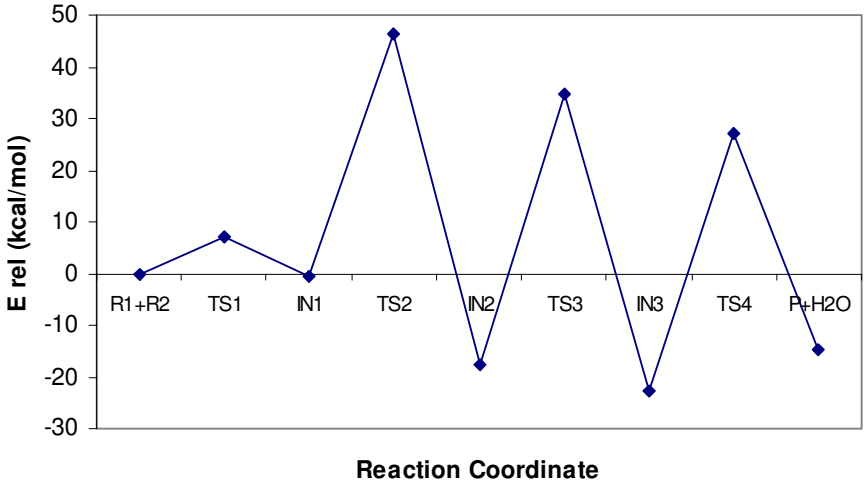

Figure 2. The energy profile of the reaction mechanism.

Quantum chemical calculations are used to explain the reaction mechanism, and the results enabled us to suggest that the reaction of **R1** with **R2** proceeded through some transition stages with intermediate

formations and a substantial role in the analysis of the paths of the reactions belongs to the interaction of frontier orbitals of reactants. According to the calculations carried out, the theoretical data support the experimental results.

Acknowledgment

This study was supported financially by the Research Foundation of Erciyes University (Kayseri, Turkey).

References

1. A. Coelho, E. Sotelo, N. Fraiz, M. Yanez and R. Laguna, **Bioorg. Med. Chem. Lett.**, **14**, 321 (2004).
2. A.D. Rawlings, B.P. Slingsby, D.G. Smith and R.W. Ward, **Bioorg. Med. Chem. Lett.**, **13**, 1581 (2003).
3. A. Deeb, F. El-Mariahb and M. Hosnyb, **Bioorg. Med. Chem. Lett.**, **14**, 5013 (2004).
4. E. Terpetschnig, W. Ott, G. Kollenz, K. Peters, E.M. Peters and H.G. von Schnering, **Monatsch Chem.**, **119**, 367-378 (1988).
5. Y. Akçamur, G. Penn, E. Ziegler, H. Sterk, G. Kollenz, K. Peters, E.M. Peters and H.G. von Schnering, **Monatsch Chem.**, **117**, 231-245 (1986).
6. G. Kollenz, E. Ziegler, W. Ott and H. Igel, **Z. Naturforschg**, **31B**, 1511-1514 (1976).
7. W. Ott, E. Ziegler and G. Kollenz, **Synthesis**, **7**, 477-478 (1976).
8. G. Kollenz, **Liebigs Ann. Chem.**, **762**, 13-22 (1972).
9. A.N. Maslivets, L.I. Smirnova and Y.S. Andreichikov, **Zh. Org. Khim.**, **24**, 1565-2205 (1988).
10. V.P. Kruglenko, V.P. Gnidets, N.A. Klynev and M.V. Povstyano, **Khim. Getersikl. Soedin.**, **4**, 533 (1987).
11. A.P. Kozlov, V.I. Svchev and Y.S. Andreichikov, **Zh. Org. Khim.**, **22**, 1756 (1986).
12. Y.S. Andreichikov, D.D. Nekrasov, M.A. Rudenko and A.Y. Konovalov, **Khim. Geterosikl. Soedin.**, **6**, 740 (1987).
13. I. Yildirim and F. Kandemirli, **Heteroatom Chem.**, **15**, 9-14 (2004).
14. Y. Akçamur, B. Altural, E. Sarıpınar, G. Kollenz, O. Kappe, K. Peters, E.M. Peters and H.G. von Schnering, **J. Heterocycl. Chem.**, **25**, 1419-1422 (1988).
15. B. Altural, Y. Akçamur, E. Sarıpınar, I. Yıldırım and G. Kollenz, **Monatsch Chem.**, **120**, 1015-1020 (1989).
16. B. Altural and G. Kollenz, **Monatsch Chem.**, **121**, 677 (1990).
17. M. Akkurt, A. Güldeste, H. Soylu, B. Altural and E. Sarıpınar, **Acta Cryst.**, **C48**, 315 (1992).
18. J.J.P. Stewart, **J. Comp. Chem.**, **10**, 209 (1989).
19. PC Spartan Pro., Wavefunction, Inc.; Irvine, California, 1999.